

Transmutation of interacting quintessence in the late universe

Amin Aboubrahim^{1,*} and Pran Nath^{2,†}

¹*Department of Physics and Astronomy, Union College,
807 Union Street, Schenectady, NY 12308, U.S.A.*

²*Department of Physics, Northeastern University,
111 Forsyth Street, Boston, MA 02115-5000, U.S.A.*

(Dated: November 19, 2024)

It is shown that the presence of an interaction between dark energy and dark matter can induce a transmutation of quintessence from thawing to scaling freezing. The analysis is done in a Lagrangian approach where dark energy and dark matter are treated as spin zero fields. Remarkably, with the cosmological constraints on energy densities of dark matter and dark energy, such a transmutation can occur in the late universe and searchable in accumulating cosmological data by DESI and other dark energy-related experiments. We give a fit to the dark energy equation of state which can be used by experimental collaborations to search for this transmutation that can occur at redshifts up to $z = 13$ depending on the interaction strength. A transmutation in the range $z = 1 - 3$ is already within reach of current and near future experiments.

Introduction: Currently the Λ CDM model is considered the Standard Model of cosmology and is successful in explaining a large amount of cosmological data. It is described by the action

$$S_{\Lambda\text{CDM}} = \int d^4x \sqrt{-g} \left[\frac{1}{16\pi G} (R - 2\Lambda) + \mathcal{L}_{\text{CDM}} \right], \quad (1)$$

where $g = \det(g^{\mu\nu})$ is the determinant of the metric $g^{\mu\nu}$. We use the FLRW metric in conformal time so that the line element is given by $ds^2 = a^2(\tau) [-d\tau^2 + g_{ij} dx^i dx^j]$, where $a(\tau)$ is the scale factor. In Eq. (1), R is the Ricci scalar, G is Newton's constant, Λ is the Einstein cosmological constant, and \mathcal{L}_{CDM} is the Lagrangian density for Cold Dark Matter (CDM). More generally, \mathcal{L}_{CDM} can be replaced by the Lagrangian density \mathcal{L}_m which includes all forms of matter and radiation. In spite of the great success of Eq. (1), some anomalies have recently emerged, with two of the prominent ones being the Hubble tension, H_0 , and the degree of matter clustering, S_8 [1]. Several suggestions to reduce the Hubble tension have been proposed which, to name a few, include interacting dark matter models [2–26], early dark energy [27, 28], decaying dark matter [29, 30] as well as models introducing extra relativistic degrees of freedom [31–38]. A [current](#) trend is to introduce an interaction term (or a source term) between dark matter (DM) and dark energy (DE) at the level of the continuity equations [1, 15, 39, 40], so that

$$\rho'_\chi + 3\mathcal{H}(1 + w_\chi)\rho_\chi = Q, \quad (2)$$

$$\rho'_\phi + 3\mathcal{H}(1 + w_\phi)\rho_\phi = -Q. \quad (3)$$

Here ρ_χ and ρ_ϕ are the energy densities for DM and DE, w_χ and w_ϕ are the corresponding equations of state

(EoS), with w defined as the ratio of pressure (p) to energy density (ρ) for a given species, $w = p/\rho$, and $' \equiv d/d\tau$. However, in Eqs. (2) and (3), the energy conservation is imposed in an ad hoc manner by choosing the sources to be $+Q$ and $-Q$ and these equations are inconsistent within a field theoretic framework.

Quintessence is a well known alternative to the cosmological constant and many models have been proposed which achieve a negative equation of state for DE at current time. Thus in thawing quintessence [41, 42], the field is initially frozen due to the Hubble friction so that $w_\phi \simeq -1$. The mass of the field then becomes smaller than \mathcal{H} at late times causing a deviation of w_ϕ away from -1 . In freezing models, w_ϕ decreases towards -1 at late times because of the shallow nature of the potential which, for a scaling freezing model [43, 44], is taken to be a double exponential potential.

In this Letter, we drop Eqs. (2) and (3) which are inconsistent within a field theoretic framework and consider a field theoretic formulation where energy conservation is automatic. We show that in this framework DM-DE interaction can lead to a transmutation of quintessence from thawing to scaling freezing. Depending on the interaction strength between DM and DE, this transmutation can occur anywhere up to $z = 13$. We give a fit to the DE equation of state which models this transmutation and propose that DESI [45] and other future cosmological probes can search for DM-DE interaction by looking for a transition redshift between the two quintessence modes at late times.

QCDM: In the analysis here we propose an alternative to Λ CDM of Eq. (1) which is a model of quintessence interacting with dark matter (QCDM) based on a Lagrangian. Thus we consider a set of n interacting spin zero fields ϕ_i ($i = 1 \dots n$) where one of the fields is the quintessence field and the rest are matter fields which may contain one or more dark matter fields and the rest may be other forms of matter fields. The action of this

* Email: abouibra@union.edu;

† Email: p.nath@northeastern.edu

theory is given by

$$S_{\text{QCDM}} = \int d^4x \sqrt{-g} \left[\frac{1}{16\pi G} R + \mathcal{L}_{\text{QCDM}} \right], \quad (4)$$

$$\mathcal{L}_{\text{QCDM}} = \sum_i \frac{1}{2} \phi_i'^{\mu} \phi_{i,\mu} - V(\{\phi_i\}, \{\phi_j\}), \quad (5)$$

$$V = \sum_i^n V_i(\phi_i) + V_{\text{int}}(\{\phi_i\}, \{\phi_j\}), \quad (6)$$

$$V_{\text{int}}(\{\phi_i\}, \{\phi_j\}) = \frac{1}{2} \sum_{i \neq j} \sum_j V_{ij}(\phi_i, \phi_j), \quad (7)$$

where $V_{ij}(\phi_i, \phi_j)$ is the interaction potential between the fields ϕ_i and ϕ_j . The Klein-Gordon equation for the field ϕ_i is given by

$$\phi_i'' + 2\mathcal{H}\phi_i' + a^2 \left(V_{i,\phi_i} + \frac{1}{2} \sum_{j \neq i} (V_{ij} + V_{ji}, \phi_i) \right) = 0, \quad (8)$$

where $V_{ij,\phi_i} \equiv \partial_{\phi_i} V_{ij}$, and $\mathcal{H} = a'/a$ is the Hubble parameter. Assuming $V_{ji} = V_{ij}$, the corresponding continuity equations are then given by

$$\rho_i' + 3\mathcal{H}(1 + w_i)\rho_i = Q_i, \quad (9)$$

$$Q_i = \sum_{j \neq i} V_{ij,\phi_j}(\phi_i, \phi_j)\phi_j'. \quad (10)$$

Here the energy density ρ_i and the pressure p_i for the energy density of field ϕ_i are given by

$$\rho_i(p_i) = T_i \pm V_i(\phi_i) \pm \sum_{j \neq i} V_{ij}(\phi_i, \phi_j), \quad (11)$$

where $+$ ($-$) are for the cases ρ_i (p_i), and $w_i = p_i/\rho_i$. The total energy density is then defined by

$$\rho = \sum_i \rho_i - \sum_{i < j} V_{ij}(\phi_i, \phi_j), \quad (12)$$

where the last term on the right hand side is included to ensure no double counting. Eq. (12) is a generalization of the two-field case [46] to the case of n -interacting fields. The observed relic density for the particle i is given by

$$\Omega_{0i} = \frac{\rho_i}{\rho_{0,\text{crit}}}(1 - \delta_i), \quad \sum_i \Omega_{0i} = 1, \quad \delta_i = \frac{\sum_{j \neq i} V_{ij}}{\sum_j \rho_j}. \quad (13)$$

Eqs. (9) and (10) are a consistent set of continuity equations for the case of n number of interacting fields, where the energy density ρ_i corresponds to the field ϕ_i .

Field-theoretic inconsistency of the fluid equation model with $\sum_i Q_i = 0$: In order to include interactions, the phenomenological fluid model uses the continuity equations of the Λ CDM model but includes interactions by assuming a set of ad hoc sources for them. To achieve conservation of energy, one then assumes that

$\rho = \sum_i \rho_i$ and imposes the condition that the sum of the sources vanishes, i.e., $\sum_i Q_i = 0$ which implies using Eq. (9) without knowledge of Eq. (10). In field theory, $\sum_i Q_i = 0$ leads to

$$V'_{\text{int}}(\{\phi_i\}, \{\phi_j\}) = 0, \quad (14)$$

which means that V_{int} is a constant (independent of time). This is obviously incorrect since it depends on n number of fields each of which is time-dependent and there is no reason why $V_{\text{int}}(\phi_i, \phi_j)$ would be independent of time. We illustrate this with an example of two interacting fields χ and ϕ with potentials

$$V_1(\chi) = m_\chi^2 f^2 \left[1 + \cos\left(\frac{\chi}{f}\right) \right], \quad (15)$$

$$V_2(\phi) = \mu^4 \left[1 + \cos\left(\frac{\phi}{F}\right) \right], \quad (16)$$

$$V_{12}(\phi, \chi) = \frac{\lambda}{2} \chi^2 \phi^2, \quad (17)$$

one of which (χ) will act as dark matter and the other (ϕ) as dark energy or quintessence [42, 47, 48]. In this case Q_χ and Q_ϕ are given by

$$Q_\chi = V_{12,\phi}\phi', \quad Q_\phi = V_{12,\chi}\chi'. \quad (18)$$

From Eq. (14), we have $V'_{12}(\chi, \phi) = 0$, i.e., $V_{12}(\chi, \phi)$ is independent of time and so we write

$$V_{12}(\chi, \phi) = \frac{\lambda}{2} \chi^2 \phi^2 = c. \quad (19)$$

Here c is a constant which gives $\chi = \pm \sqrt{\frac{2c}{\lambda}} \phi$, i.e., the fields χ and ϕ are not independent but one is determined in terms of the other which is obviously false. Thus the fluid equations, Eq. (2) and Eq. (3), are inconsistent within a field theoretic framework.

Cosmological evolution of interacting dark energy and dark matter in QCDM: Before giving an analysis of the transmutation phenomenon from thawing to scaling freezing, we discuss first the evolution of some background cosmological parameters obtained using a modified version of CLASS [49]. In order to overcome numerical difficulties arising from the rapid oscillations of the DM field once $\mathcal{H}/m_\chi \ll 1$ [50], we use angular variables [23, 44] defined in the supplementary material to help absorb these fast oscillations. In Fig. 1, we show in the upper left panel the energy densities of baryons, photons, DM and DE while in the upper right panel the EoS of DM and DE are shown as well as the total EoS. In both panels, the evolutions of ρ and w are for three values of ϕ_{ini} and μ^4 , where similar to Λ CDM, the QCDM model predicts the redshift of matter-radiation equality to be $z_{\text{eq}} \sim 3390$ consistent with Planck's measurements. Now examining the upper right panel for the EoS, we note that at early times, $w_\chi = -1$ and $w_\phi = +1$ and

so the ϕ field acts as radiation while the χ field acts as an early DE component for a period of time before the onset of rapid oscillations at around $a \sim 10^{-5}$. Averaging the fast oscillations in χ renders $w_\chi = 0$ and so the χ field eventually dilutes as CDM, i.e., $\rho_\chi \sim a^{-3}$. The ϕ field, on the other hand, starts off as radiation and as the DE potential rolls down to its minimum, the EoS drops to -1 . The interesting feature here is that similar to χ , the DE field begins to oscillate but at a later time, around $a \sim 10^{-2}$. The difference between the oscillations of the χ and ϕ fields is that while the amplitude of oscillations of w_χ is constant, that of ϕ is decaying. Averaging over these oscillations, we display in Fig. 1 the variations in w_ϕ where one can see w_ϕ departing away from -1 before turning around and decreasing again toward -1 . One finds that for $\phi_{\text{ini}} = 0.1$, w_ϕ decays to -1 as one would expect from a DE component, while for $\phi_{\text{ini}} = 0.5$, $w_\phi \sim -0.9$. However, for $\phi_{\text{ini}} = 1.0$, the oscillations remain strong even at $a = 1$ and even though the averaged w_ϕ is less than zero, it is still much larger than -1 , which is the well accepted value from observations. We show in the bottom panels Fig. 1 the allowed regions of the parameter space in the λ - F plane where the hashed area is excluded by DESI results [45] based on the DE EoS at $a = 1$ and the region bounded by the brown contour is excluded based on the H_0 value. The color axis represents the matter density fraction and the stars in each of the two panels correspond to benchmarks that are in agreement with the full DESI results. Notice that much of the regions of matter over-density is excluded by constraints on H_0 and w_ϕ while regions of under-density remain largely unconstrained.

Transmutation of quintessence from thawing to scaling freezing: We now address the peculiar evolution of w_ϕ seen in the upper right panel of Fig. 1 for $a > 10^{-2}$. To do so, we consider the DE equation of state close to scale factor $a = 1$ and discuss how the results compare to the latest DESI observations. DESI considers two parameterizations for the DE equation of state, where for the first case $w_\phi = \text{constant}$ (labeled as $w\text{CDM}$) and for the second case the parametrization $w(a) = w_0 + w_a(1 - a)$ is used (labeled as $w_0w_a\text{CDM}$). In Fig. 2, we exhibit the evolution of the DE EoS between $a = 0.1$ and $a = 1$ for the case of no DM-DE interaction (left) and when DM-DE interaction is switched on (right). The green band shows the 1σ range of the allowed values of w_ϕ as obtained from the combination of the data set DESI + CMB + PantheonPlus under the $w\text{CDM}$ assumption, while the blue band is the 1σ range under the $w_0w_a\text{CDM}$ assumption. In the absence of DM-DE interaction, the EoS tracks $w_\phi = -1$ before it starts to deviate away from it close to $a = 0.3$ which is consistent with thawing models with a pseudo-Nambu-Goldstone boson potential [51]. The benchmark in red is consistent with the DESI $w\text{CDM}$ result (green band), while the other two benchmarks (blue and or-

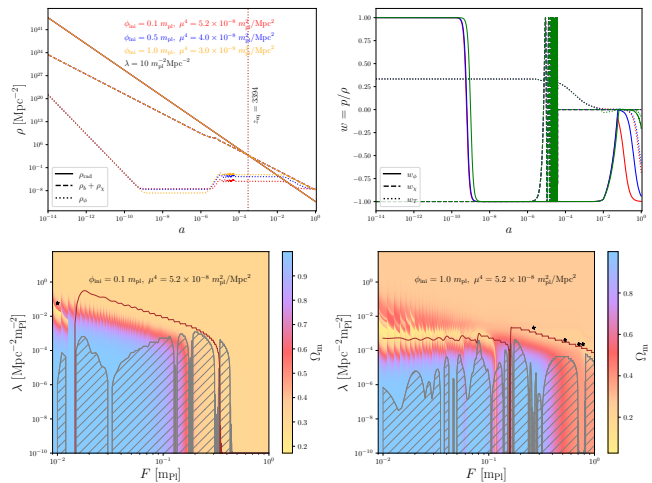


FIG. 1. Top panels: Plots of the energy densities (left) and the equations of state (right) as a function of the scale factor a for three values of ϕ_{ini} and μ^4 in the presence of DM-DE interaction. Bottom panels: Variation of the matter density Ω_m (color axis) in the λ - F plane for two values of ϕ_{ini} (left and right panels). The hatched regions are excluded by DESI constraints on w_ϕ and the stars represent points satisfying $\Omega_m \sim 0.3$ as measured by DESI. The regions enclosed by the brown contours are excluded due to constraints on H_0 .

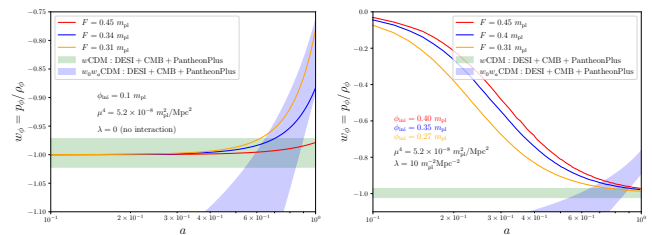


FIG. 2. A plot of the EoS of ϕ as a function of the scale factor a exhibiting the thawing behavior (left) when $\lambda = 0$ and scaling freezing (right) when $\lambda \neq 0$.

ange) are consistent with the $w_0w_a\text{CDM}$ prediction near $a = 1$. Note that this comparison is not meant to try and extract constraints on the $Q\text{CDM}$ model parameters based on DESI's results. DESI's $w_0w_a\text{CDM}$ parameterization leads to the DE EoS crossing the phantom divide, something that quintessence does not predict¹. When the DM-DE interaction is switched on (right panel), we notice that the dynamics of the EoS changes significantly. The evolution of w_ϕ becomes consistent with scaling freezing models [44, 55], where the EoS slowly approaches $w_\phi = -1$ as $a \rightarrow 1$. Therefore, the presence of the interaction term has modified the DE potential in such a way that the new behavior

¹ Fits to DESI results have been carried out recently for quintessence, e.g. in refs. [52–54].

now resembles that of scaling freezing models with an evolution that fits well a double exponential potential $V(\phi) = \tilde{V}_0(e^{-\lambda_1\phi} + e^{-\lambda_2\phi})$. Note that both the thawing and scaling freezing modes pertaining to w_ϕ appear in the upper right panel of Fig. 1 where there is a clear transition from thawing to scaling freezing near $a_t \sim 0.1$ for non-zero interaction. Analytically, one can see this behavior by expanding the potentials around the minimum, so that $V_2(\phi) + V_{12}(\phi, \chi) = \mu^4[1 + \cos(\phi/F)] + \lambda\chi^2\phi^2/2 \simeq 2\mu^4 + V_0\phi^2$, where $V_0 = (\lambda\chi^2/2 - \mu^4/2F^2)$. Fitting the QCDM model data to the double exponential potential, we find that $\lambda_1 = -\lambda_2$, and so $V(\phi) = \tilde{V}_0(e^{-\lambda_1\phi} + e^{\lambda_1\phi}) = 2\tilde{V}_0 \cosh(\lambda_1\phi) \simeq 2\tilde{V}_0 + \tilde{V}_0\lambda_1^2\phi^2$. Notice that the two equations describe the same physics which explains the transition between thawing and scaling freezing quintessence.

To directly observe whether there is a correlation between the transition scale factor a_t and the interaction strength λ , we run a Monte Carlo analysis of the QCDM model and exhibit the correlation density plots in Fig. 3 for some variables of interest. One can clearly see the strong negative correlation ($r = -0.95$) between $\log \lambda$ and $\log a_t$ confirming that for larger λ the transition happens earlier, i.e. $a < 1$. A strong positive correlation is observed between H_0 and ϕ_{ini} on one hand and w_ϕ and ϕ_{ini} on the other. Further, a very weak correlation exists between H_0 and λ which means that alleviating the Hubble tension using the interaction $\lambda\chi^2\phi^2/2$ is unlikely as was also shown in an earlier work [46]. However, the presence of such an interaction may be inferred from the thawing to scaling freezing transition described above. Note that the DESI data can accommodate both models but direct observation from data of such a transition can be a clear sign of a DM-DE interaction.

In Fig. 4, we show the evolution of the DE equation of state as a function of the redshift $z = 1/a - 1$ for five values of the interaction strength λ (solid curves) with the dashed curves representing the fits to the data from the QCDM model. The fit is given by

$$w(a) = -1 + \frac{\alpha a^p e^{-p a}}{1 + (\beta a)^q}, \quad (20)$$

where α , β , p and q are the fit parameters. The transition from thawing to scaling freezing can be determined by numerically solving the equation for a_t using $a_t + \beta^q a_t^q \left(\frac{q}{p} + a_t - 1 \right) - 1 = 0$. For the five values of λ shown in Fig. 4, we get the transition redshifts from the fit to be $z_t = 1.615 \pm 0.006$, $z_t = 2.300 \pm 0.004$, $z_t = 2.963 \pm 0.004$, $z_t = 4.819 \pm 0.011$ and $z_t = 8.82 \pm 0.24$, respectively. Thus, a smaller a_t (or a larger z_t) corresponds to a stronger interaction strength. The parameterization of the EoS given by Eq. (20) can be used by experimental collaborations to test whether such a transition exists. A value of $z_t > 1$ will be a sign of a DM-DE interaction affecting late EoS evolution. In addition to tests at DES, transmutation from thawing to scaling

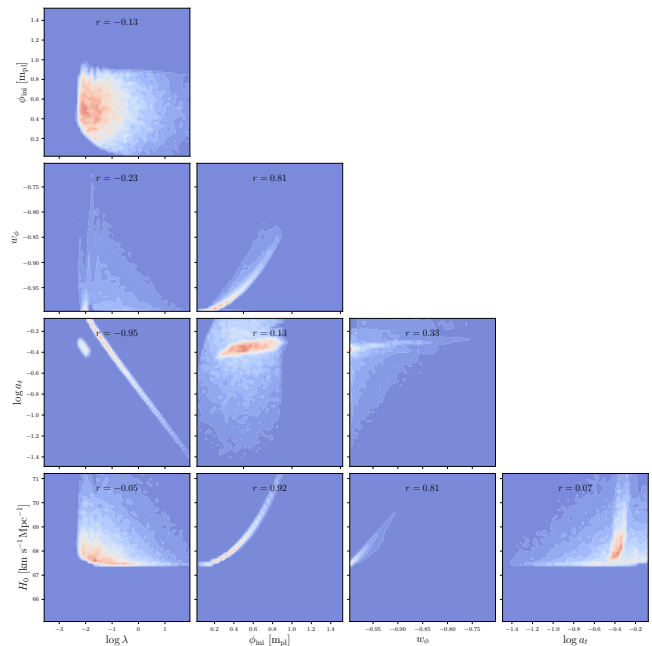


FIG. 3. Triangle density plots of a few input and output variables with the Pearson correlation coefficient r shown for each pair of variables.

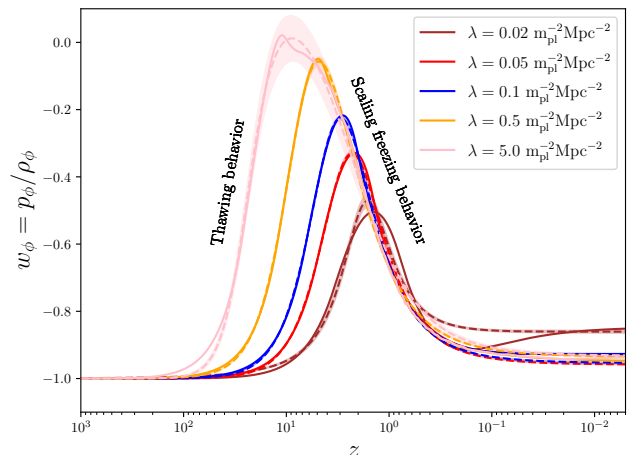


FIG. 4. Evolution of w_ϕ for quintessence for five values of λ as a function of the redshift z . The solid lines are w_ϕ predicted by QCDM and the dashed lines are fits based on Eq. (20) including a 1σ error band around each curve. In each case, quintessence transmutes from thawing (left shoulder) to scaling freezing (right shoulder) induced by λ .

freezing can be tested at Euclid [56] ($z = 0.7 - 2.0$), at Vera C. Rubin Observatory [57] ($z = 0 - 3.0$), eBOSS ($z = 0.6 - 2.2$) and at JWST ($z = 0 - 2.0$).

Conclusion: In addition to reproducing the correct cosmology, the QCDM model predicts a transition from thawing to scaling freezing quintessence which is a direct result of the DM-DE interaction term. It is shown that

the transmutation can occur in a wide range of redshifts from very low z up to $z = 13$. Thus a part of the region up to redshifts of $z = 3.0$ can be probed by DESI and other current and future experiments measuring the DE equation of state. The observation of transmutation will be direct evidence of dark energy-dark matter interaction and can provide a measure of its strength.

Acknowledgments

A communication with Kyle S. Dawson is acknowledged. The research of PN was supported in part by the NSF Grant PHY-2209903. The analysis presented here was done using the computing resources of the Phage Cluster at Union College.

-
- [1] E. Abdalla, G. Franco Abellán, A. Aboubrahim, A. Agnello, O. Akarsu, Y. Akrami, G. Alestas, D. Aloni, L. Amendola and L. A. Anchordoqui, *et al.* *JHEAp* **34**, 49-211 (2022) doi:10.1016/j.jheap.2022.04.002 [arXiv:2203.06142 [astro-ph.CO]].
- [2] A. Pourtsidou, C. Skordis and E. J. Copeland, *Phys. Rev. D* **88**, no.8, 083505 (2013) doi:10.1103/PhysRevD.88.083505 [arXiv:1307.0458 [astro-ph.CO]].
- [3] A. Pourtsidou and T. Tram, *Phys. Rev. D* **94**, no.4, 043518 (2016) doi:10.1103/PhysRevD.94.043518 [arXiv:1604.04222 [astro-ph.CO]].
- [4] M. S. Linton, A. Pourtsidou, R. Crittenden and R. Maartens, *JCAP* **04**, 043 (2018) doi:10.1088/1475-7516/2018/04/043 [arXiv:1711.05196 [astro-ph.CO]].
- [5] F. N. Chamings, A. Avgoustidis, E. J. Copeland, A. M. Green and A. Pourtsidou, *Phys. Rev. D* **101**, no.4, 043531 (2020) doi:10.1103/PhysRevD.101.043531 [arXiv:1912.09858 [astro-ph.CO]].
- [6] S. Pan, W. Yang, E. Di Valentino, E. N. Saridakis and S. Chakraborty, *Phys. Rev. D* **100**, no.10, 103520 (2019) doi:10.1103/PhysRevD.100.103520 [arXiv:1907.07540 [astro-ph.CO]].
- [7] M. Bonici and N. Maggiore, *Eur. Phys. J. C* **79**, no.8, 672 (2019) doi:10.1140/epjc/s10052-019-7198-1 [arXiv:1812.11176 [gr-qc]].
- [8] W. Yang, O. Mena, S. Pan and E. Di Valentino, *Phys. Rev. D* **100**, no.8, 083509 (2019) doi:10.1103/PhysRevD.100.083509 [arXiv:1906.11697 [astro-ph.CO]].
- [9] S. Pan, G. S. Sharov and W. Yang, *Phys. Rev. D* **101**, no.10, 103533 (2020) doi:10.1103/PhysRevD.101.103533 [arXiv:2001.03120 [astro-ph.CO]].
- [10] B. Wang, E. Abdalla, F. Atrio-Barandela and D. Pavon, *Rept. Prog. Phys.* **79**, no.9, 096901 (2016) doi:10.1088/0034-4885/79/9/096901 [arXiv:1603.08299 [astro-ph.CO]].
- [11] B. Wang, E. Abdalla, F. Atrio-Barandela and D. Pavón, *Rept. Prog. Phys.* **87**, no.3, 036901 (2024) doi:10.1088/1361-6633/ad2527 [arXiv:2402.00819 [astro-ph.CO]].
- [12] C. G. Boehmer, N. Tamanini and M. Wright, *Phys. Rev. D* **91**, no.12, 123002 (2015) doi:10.1103/PhysRevD.91.123002 [arXiv:1501.06540 [gr-qc]].
- [13] C. G. Boehmer, N. Tamanini and M. Wright, *Phys. Rev. D* **91**, no.12, 123003 (2015) doi:10.1103/PhysRevD.91.123003 [arXiv:1502.04030 [gr-qc]].
- [14] W. J. Potter and S. Chongchitnan, *JCAP* **09**, 005 (2011) doi:10.1088/1475-7516/2011/09/005 [arXiv:1108.4414 [astro-ph.CO]].
- [15] E. Di Valentino, A. Melchiorri, O. Mena and S. Vagnozzi, *Phys. Rev. D* **101**, no.6, 063502 (2020) doi:10.1103/PhysRevD.101.063502 [arXiv:1910.09853 [astro-ph.CO]].
- [16] E. Di Valentino, A. Melchiorri, O. Mena and S. Vagnozzi, *Phys. Dark Univ.* **30**, 100666 (2020) doi:10.1016/j.dark.2020.100666 [arXiv:1908.04281 [astro-ph.CO]].
- [17] L. A. Escamilla, O. Akarsu, E. Di Valentino and J. A. Vazquez, *JCAP* **11**, 051 (2023) doi:10.1088/1475-7516/2023/11/051 [arXiv:2305.16290 [astro-ph.CO]].
- [18] A. Bernui, E. Di Valentino, W. Giarè, S. Kumar and R. C. Nunes, *Phys. Rev. D* **107**, no.10, 103531 (2023) doi:10.1103/PhysRevD.107.103531 [arXiv:2301.06097 [astro-ph.CO]].
- [19] W. Yang, S. Pan, O. Mena and E. Di Valentino, *JHEAp* **40**, 19-40 (2023) doi:10.1016/j.jheap.2023.09.001 [arXiv:2209.14816 [astro-ph.CO]].
- [20] L. Amendola, *Phys. Rev. D* **62**, 043511 (2000) doi:10.1103/PhysRevD.62.043511 [arXiv:astro-ph/9908023 [astro-ph]].
- [21] R. Kase and S. Tsujikawa, *Phys. Rev. D* **101**, no.6, 063511 (2020) doi:10.1103/PhysRevD.101.063511 [arXiv:1910.02699 [gr-qc]].
- [22] P. Pérez, U. Nucamendi and R. De Arcia, *Eur. Phys. J. C* **81**, no.12, 1063 (2021) doi:10.1140/epjc/s10052-021-09857-4 [arXiv:2104.07690 [gr-qc]].
- [23] G. Garcia-Arroyo, L. A. Ureña-López and J. A. Vázquez, *Phys. Rev. D* **110**, no.2, 023529 (2024) doi:10.1103/PhysRevD.110.023529 [arXiv:2402.08815 [astro-ph.CO]].
- [24] J. Beyer, S. Nurmi and C. Wetterich, *Phys. Rev. D* **84**, 023010 (2011) doi:10.1103/PhysRevD.84.023010 [arXiv:1012.1175 [astro-ph.CO]].
- [25] J. Beyer, [arXiv:1407.0497 [astro-ph.CO]].
- [26] C. van de Bruck, G. Poulot and E. M. Teixeira, *JCAP* **07**, 019 (2023) doi:10.1088/1475-7516/2023/07/019 [arXiv:2211.13653 [hep-th]].
- [27] M. Doran and G. Robbers, *JCAP* **06**, 026 (2006) doi:10.1088/1475-7516/2006/06/026 [arXiv:astro-ph/0601544 [astro-ph]].
- [28] P. Agrawal, F. Y. Cyr-Racine, D. Pinner and L. Randall, *Phys. Dark Univ.* **42**, 101347 (2023) doi:10.1016/j.dark.2023.101347 [arXiv:1904.01016 [astro-ph.CO]].
- [29] Z. Berezhiani, A. D. Dolgov and I. I. Tkachev, *Phys. Rev. D* **92**, no.6, 061303 (2015) doi:10.1103/PhysRevD.92.061303 [arXiv:1505.03644 [astro-ph.CO]].
- [30] A. Ibarra, D. Tran and C. Weniger, *Int. J. Mod. Phys. A* **28**, 1330040 (2013) doi:10.1142/S0217751X13300408 [arXiv:1307.6434 [hep-ph]].

- [31] A. Aboubrahim, M. Klasen and P. Nath, *JCAP* **04**, no.04, 042 (2022) doi:10.1088/1475-7516/2022/04/042 [arXiv:2202.04453 [astro-ph.CO]].
- [32] E. Fernandez-Martinez, M. Pierre, E. Pinsard and S. Rosauero-Alcaraz, *Eur. Phys. J. C* **81**, no.10, 954 (2021) doi:10.1140/epjc/s10052-021-09760-y [arXiv:2106.05298 [hep-ph]].
- [33] M. Escudero and S. J. Witte, *Eur. Phys. J. C* **81**, no.6, 515 (2021) doi:10.1140/epjc/s10052-021-09276-5 [arXiv:2103.03249 [hep-ph]].
- [34] D. Baumann, D. Green, J. Meyers and B. Wallisch, *JCAP* **01**, 007 (2016) doi:10.1088/1475-7516/2016/01/007 [arXiv:1508.06342 [astro-ph.CO]].
- [35] C. Brust, Y. Cui and K. Sigurdson, *JCAP* **08**, 020 (2017) doi:10.1088/1475-7516/2017/08/020 [arXiv:1703.10732 [astro-ph.CO]].
- [36] N. Blinov and G. Marques-Tavares, *JCAP* **09**, 029 (2020) doi:10.1088/1475-7516/2020/09/029 [arXiv:2003.08387 [astro-ph.CO]].
- [37] T. D. Jacques, L. M. Krauss and C. Lunardini, *Phys. Rev. D* **87**, no.8, 083515 (2013) [erratum: *Phys. Rev. D* **88**, no.10, 109901 (2013)] doi:10.1103/PhysRevD.87.083515 [arXiv:1301.3119 [astro-ph.CO]].
- [38] A. J. Cuesta, M. E. Gómez, J. I. Illana and M. Masip, *JCAP* **04**, no.04, 009 (2022) doi:10.1088/1475-7516/2022/04/009 [arXiv:2109.07336 [hep-ph]].
- [39] J. Valiviita, E. Majerotto and R. Maartens, *JCAP* **07**, 020 (2008) doi:10.1088/1475-7516/2008/07/020 [arXiv:0804.0232 [astro-ph]].
- [40] M. B. Gavela, D. Hernandez, L. Lopez Honorez, O. Mena and S. Rigolin, *JCAP* **07**, 034 (2009) [erratum: *JCAP* **05**, E01 (2010)] doi:10.1088/1475-7516/2009/07/034 [arXiv:0901.1611 [astro-ph.CO]].
- [41] R. J. Scherrer and A. A. Sen, *Phys. Rev. D* **77**, 083515 (2008) doi:10.1103/PhysRevD.77.083515 [arXiv:0712.3450 [astro-ph]].
- [42] R. R. Caldwell and E. V. Linder, *Phys. Rev. Lett.* **95**, 141301 (2005) doi:10.1103/PhysRevLett.95.141301 [arXiv:astro-ph/0505494 [astro-ph]].
- [43] P. G. Ferreira and M. Joyce, *Phys. Rev. D* **58**, 023503 (1998) doi:10.1103/PhysRevD.58.023503 [arXiv:astro-ph/9711102 [astro-ph]].
- [44] E. J. Copeland, A. R. Liddle and D. Wands, *Phys. Rev. D* **57**, 4686-4690 (1998) doi:10.1103/PhysRevD.57.4686 [arXiv:gr-qc/9711068 [gr-qc]].
- [45] A. G. Adame *et al.* [DESI], [arXiv:2404.03002 [astro-ph.CO]].
- [46] A. Aboubrahim and P. Nath, *JCAP* **09**, 076 (2024) doi:10.1088/1475-7516/2024/09/076 [arXiv:2406.19284 [astro-ph.CO]].
- [47] G. Pantazis, S. Nesseris and L. Perivolaropoulos, *Phys. Rev. D* **93**, no.10, 103503 (2016) doi:10.1103/PhysRevD.93.103503 [arXiv:1603.02164 [astro-ph.CO]].
- [48] S. Tsujikawa, *Class. Quant. Grav.* **30**, 214003 (2013) doi:10.1088/0264-9381/30/21/214003 [arXiv:1304.1961 [gr-qc]].
- [49] D. Blas, J. Lesgourgues and T. Tram, *JCAP* **07**, 034 (2011) doi:10.1088/1475-7516/2011/07/034 [arXiv:1104.2933 [astro-ph.CO]].
- [50] M. S. Turner, *Phys. Rev. D* **28**, 1243 (1983) doi:10.1103/PhysRevD.28.1243
- [51] J. A. Frieman, C. T. Hill, A. Stebbins and I. Waga, *Phys. Rev. Lett.* **75**, 2077-2080 (1995) doi:10.1103/PhysRevLett.75.2077 [arXiv:astro-ph/9505060 [astro-ph]].
- [52] Y. Tada and T. Terada, *Phys. Rev. D* **109**, no.12, L121305 (2024) doi:10.1103/PhysRevD.109.L121305 [arXiv:2404.05722 [astro-ph.CO]].
- [53] J. Rebouças, D. H. F. de Souza, K. Zhong, V. Miranda and R. Rosenfeld, [arXiv:2408.14628 [astro-ph.CO]].
- [54] K. V. Berghaus, J. A. Kable and V. Miranda, [arXiv:2404.14341 [astro-ph.CO]].
- [55] P. G. Ferreira and M. Joyce, *Phys. Rev. Lett.* **79**, 4740-4743 (1997) doi:10.1103/PhysRevLett.79.4740 [arXiv:astro-ph/9707286 [astro-ph]].
- [56] R. Laureijs *et al.* [EUCLID], [arXiv:1110.3193 [astro-ph.CO]].
- [57] Ž. Ivezić *et al.* [LSST], *Astrophys. J.* **873**, no.2, 111 (2019) doi:10.3847/1538-4357/ab042c [arXiv:0805.2366 [astro-ph]].
- [58] L. A. Ureña-López and A. X. Gonzalez-Morales, *JCAP* **07**, 048 (2016) doi:10.1088/1475-7516/2016/07/048 [arXiv:1511.08195 [astro-ph.CO]].

Transmutation of interacting quintessence in the late universe

Supplemental Material

Amin Aboubrahim and Pran Nath

Here we give further details of the analysis presented in the Letter where we discuss the background equations used and further numerical analysis. Thus, we present all the Klein-Gordon equations as well as the dark matter background equations rewritten in terms of angular variables that are used to evolve the background cosmology of the Λ CDM model. We also give the background equations of the phenomenological model resulting from the $\sum_i Q_i = 0$ assumption for the sake of comparison with Λ CDM. In order to explain the reason behind the transmutation from thawing to scaling freezing quintessence in the late universe, we show the fit to the total potential using a double exponential potential. The latter leads to what is known as scaling freezing behavior.

Background equations and angular variables

The interacting quintessence-dark matter model (QCDM) represents an alternative to Λ CDM. In the notation used in the Letter, χ is a dark matter field while ϕ is a dark energy field governed by the potentials given by

$$V_1(\chi) = m_\chi^2 f^2 \left[1 + \cos\left(\frac{\chi}{f}\right) \right], \quad (\text{S1})$$

$$V_2(\phi) = \mu^4 \left[1 + \cos\left(\frac{\phi}{F}\right) \right]. \quad (\text{S2})$$

The interaction potential between χ and ϕ is based on field theory and is given by

$$V_{12}(\phi, \chi) = \frac{\lambda}{2} \chi^2 \phi^2. \quad (\text{S3})$$

We track the evolution of the two background fields χ and ϕ fields by solving the Klein-Gordon (KG) equations

$$\chi_0'' + 2\mathcal{H}\chi_0' + a^2(V_{1,\chi} + V_{12,\chi}) = 0, \quad (\text{S4})$$

$$\phi_0'' + 2\mathcal{H}\phi_0' + a^2(V_{2,\phi} + V_{12,\phi}) = 0, \quad (\text{S5})$$

where a is the scale factor as a function of conformal time, $\mathcal{H} = a'/a$ and the ‘0’ subscript denotes a background field. For a DM potential of the form given by Eq. (S1), the field undergoes rapid oscillations when $\mathcal{H}/m_\chi \ll 1$, making a numerical solution intractable. In order to efficiently solve the background evolution equation for the DM field, we recast Eq. (S4) in a different form. First, let us define the DM energy density so that $\tilde{\rho}_\chi = \rho_\chi - V_{12}$ so that the modified energy density fraction becomes

$$\tilde{\Omega}_\chi \equiv \frac{\tilde{\rho}_\chi}{\rho_{\text{cr}}} = \frac{\kappa^2}{6\mathcal{H}^2} \left(\chi_0'^2 + 2a^2 V_1(\chi_0) \right), \quad (\text{S6})$$

where $\kappa \equiv \sqrt{8\pi G}$. Based on Eq. (S6), we define the following new dimensionless variables

$$\tilde{\Omega}_\chi^{1/2} \sin\left(\frac{\theta}{2}\right) = \frac{\kappa\chi'}{\sqrt{6}\mathcal{H}}, \quad (\text{S7})$$

$$\tilde{\Omega}_\chi^{1/2} \cos\left(\frac{\theta}{2}\right) = \frac{\kappa a V_1^{1/2}}{\sqrt{3}\mathcal{H}}, \quad (\text{S8})$$

$$y = -\frac{2\sqrt{2}a}{\mathcal{H}} \partial_\chi V_1^{1/2}. \quad (\text{S9})$$

The advantage in introducing the new variables is that the rapid oscillations of the DM field can be absorbed into the θ variable. As a result, the DM equation of state begins to oscillate rapidly between +1 and -1, so that the time-average of w_χ becomes zero, thus describing a pressureless fluid, i.e., CDM. To proceed further, we recast the KG equation for χ and ϕ in terms of the new variables defined by Eqs. (S7)–(S9). For the field χ after some lengthy,

but otherwise straightforward, calculation, we obtain the differential equations of $\Omega_\chi = \rho_\chi/\rho_{\text{cr}}$, θ and y . For Ω_χ we have

$$\Omega'_\chi = 3\mathcal{H}\Omega_\chi(w_T - w_\chi) + \frac{\kappa^2 a^2}{3\mathcal{H}^2} \left[\mathcal{H}(1 + 3w_\chi)V_{12} - \chi'V_{12,\chi} \right], \quad (\text{S10})$$

with the DM equation of state $w_\chi = -\cos\theta$ and $w_T = \sum p_i/\sum \rho_i$, where the sum is over all species (baryons, photons, neutrinos, DM and DE). As for the variables θ and y , we get

$$\theta' = -3\mathcal{H}\sin\theta + \mathcal{H}y - \frac{\kappa^2 a^2}{3\mathcal{H}^2 \tilde{\Omega}_\chi} \left(2\mathcal{H}V_{12} + \chi'V_{12,\chi} \right) \cot\frac{\theta}{2}, \quad (\text{S11})$$

and

$$y' = \frac{3}{2}\mathcal{H}(1 + w_T)y + \frac{\beta_\chi}{2}\mathcal{H}\tilde{\Omega}_\chi \sin\theta, \quad (\text{S12})$$

where $\beta_\chi \equiv 3/(\kappa^2 f^2)$ and $\tilde{\Omega}_\chi = \Omega_\chi - (\kappa^2 a^2/3\mathcal{H}^2)V_{12}$. Note that the last set of terms in each of Eqs. (S10) and (S11) represent the interaction term.

Next, we consider the assumption $Q_\chi = -Q_\phi$ and discuss its impact on cosmology from a field theory perspective. This assumption directly leads to $V'_{12} = 0$ so that

$$V_{12,\phi}\phi'_0 + V_{12,\chi}\chi'_0 = 0, \quad (\text{S13})$$

Differentiating Eq. (S13) with respect to time and using Eq. (S5) we get

$$V_{12,\chi\chi}\chi_0'^2 + V_{12,\chi}\chi_0'' + V_{12,\phi\phi} \left(\frac{V_{12,\chi}}{V_{12,\phi}} \right)^2 \chi_0'^2 - 2\mathcal{H}V_{12,\phi} \left(-\frac{V_{12,\chi}}{V_{12,\phi}} \chi_0' \right) - a^2 V_{12,\phi} V_{t,\phi} = 0, \quad (\text{S14})$$

where $V_t = V_2 + V_{12}$. Now let us take Eq. (S13) and differentiate one time with respect to χ

$$V_{12,\chi\chi}\chi'_0 + V_{12,\chi\phi}\phi'_0 = 0, \quad (\text{S15})$$

and then another with respect to ϕ

$$V_{12,\phi\chi}\chi'_0 + V_{12,\phi\phi}\phi'_0 = 0. \quad (\text{S16})$$

Eliminating $V_{12,\phi\chi}$ from both equations gives

$$V_{12,\chi\chi} = V_{12,\phi\phi} \left(\frac{V_{12,\chi}}{V_{12,\phi}} \right)^2. \quad (\text{S17})$$

Using this result in Eq. (S14), we get

$$\chi_0'' + 2\mathcal{H}\chi_0' + \frac{2V_{12,\chi\chi}}{V_{12,\chi}}\chi_0'^2 - a^2 \frac{V_{12,\phi}V_{t,\phi}}{V_{12,\chi}} = 0, \quad (\text{S18})$$

which is a different equation from the KG equation of χ , i.e., Eq. (S4). However, the field χ cannot obey two different KG equations. Setting Eq. (S18) equal to Eq. (S4) gives

$$\chi_0'^2 = \frac{a^2 V_{12,\chi}}{2V_{12,\chi\chi}} \left(V_{1,\chi} + V_{12,\chi} + \frac{V_{12,\phi}V_{t,\phi}}{V_{12,\chi}} \right). \quad (\text{S19})$$

Since $V_{12} = \frac{\lambda}{2}\chi^2\phi^2 = \text{constant}$ implies that $\chi^2\phi^2 = c$, where c is a constant of time. In this case, Eq. (S19) becomes

$$\chi_0'^2 = \frac{a^2}{2}\chi_0 \left(V_{1,\chi} + V_{12,\chi} + \frac{\chi_0}{\phi_0} V_{t,\phi} \right). \quad (\text{S20})$$

Using Eq. (S6), Eq. (S20) and Eqs. (S7)–(S9), we get a new set of differential equations

$$\begin{aligned}\Omega'_\chi &= 3\mathcal{H}\tilde{\Omega}_\chi(1+w_T) - \frac{5}{8}\mathcal{H}\tilde{\Omega}_\chi y \sin\theta + \frac{\kappa^2 a^2}{2\mathcal{H}}\lambda c(1+w_T) \\ &+ \frac{\sqrt{6}\kappa a^2}{12\mathcal{H}}\tilde{\Omega}_\chi^{1/2}\mathcal{V}_1 \sin\frac{\theta}{2} - \frac{\kappa^2 a^2}{12\mathcal{H}^2}c\frac{\phi'_0}{\phi_0^3}\mathcal{V}_2 - \frac{\kappa^2}{48}cY,\end{aligned}\quad (\text{S21})$$

and

$$\theta' = \frac{1}{8}\mathcal{H}y(3-5\cos\theta) + \frac{\sqrt{6}\kappa a^2}{12\mathcal{H}\tilde{\Omega}_\chi^{1/2}}\mathcal{V}_1 \cos\frac{\theta}{2} - \frac{\kappa^2 a^2}{12\mathcal{H}^2\tilde{\Omega}_\chi}c\frac{\phi'_0}{\phi_0^3}\mathcal{V}_2 \cot\frac{\theta}{2} - \frac{\kappa^2}{48\tilde{\Omega}_\chi}cY \cot\frac{\theta}{2}, \quad (\text{S22})$$

where

$$\mathcal{V}_1 = \frac{2V_{2,\phi}}{\phi_0} + \frac{2\lambda c}{\phi_0^2} - V_{2,\phi\phi}, \quad (\text{S23})$$

$$\mathcal{V}_2 = \lambda\phi_0^2 + \frac{V_{2,\phi}}{\phi_0} + \frac{\lambda c}{\phi_0^2}, \quad (\text{S24})$$

$$Y = \frac{\phi'_0}{\phi_0^3} \left[y^2 - \beta_\chi \tilde{\Omega}_\chi (1 + \cos\theta) \right]. \quad (\text{S25})$$

Here one finds that the new Eqs. (S21) and (S22) are driven by the DE potential and the solution to the KG equation of ϕ . Due to the constraint $V_{12} = \lambda c/2$, one can determine an equation for y so that

$$y = \frac{4}{\mathcal{H}}\frac{\phi'_0}{\phi_0} \tan\frac{\theta}{2} - \frac{2\kappa^2 a^2}{3\mathcal{H}^3\tilde{\Omega}_\chi \sin\theta}c\frac{\phi'_0}{\phi_0^3}\mathcal{V}_2. \quad (\text{S26})$$

We now have a set of equations to solve for the cases when Q_χ and Q_ϕ are not constrained in which case we solve Eqs. (S10), (S11) and (S12), while for the case where $Q_\chi = -Q_\phi$, we solve Eqs. (S21), (S22) and (S26). To track the evolution of the DE field, we directly solve the KG equation, Eq. (S5). We implement and solve the above equations in the Boltzmann equation solver CLASS in order to determine the evolution of the DM and DE fields as well as the SM species (photons, baryons and neutrinos). To make sure the closure relation $\sum_i \Omega_i = 1$ is satisfied, we use the shooting method in CLASS to evolve the background equations starting from $a_{\text{ini}} = 10^{-14}$ to $a_0 = 1$ (today). The shooting variable is Ω_χ and a quantity $\mathcal{O}(10^{-2})$ is varied during the shooting process in order to achieve today's DM abundance $\Omega_{\chi 0} \sim 0.26$. For the first scenario where Q_χ and Q_ϕ are unconstrained, we use the attractor initial conditions for the field χ [58], while for the second scenario where $Q_\chi + Q_\phi = 0$, the initial conditions are chosen so that the shooting method converges. For the DE field ϕ we choose the initial conditions ϕ_{ini} and $\phi'_{\text{ini}} = 10^{-3}$ and an estimate of μ^4 is determined by minimizing the DE potential so that $\mu^4 = \frac{3}{2}H_0^2\Omega_{\phi 0}$. This value serves as an initial estimate and we modify μ^4 accordingly in order to try and achieve a consistent cosmology. Furthermore, for simplicity, we set $\beta_\chi = 0$.

Comparison between QCDM and the phenomenological model

As an alternative model to Λ CDM, QCDM must be able to consistently describe our universe. We show in Fig. S1 some of the important observables and their evolution. In the top panels we exhibit the evolution of the energy density fraction (left) and of the energy density (right) for all the species and for three values of ϕ_{ini} and μ^4 for the case of non-zero DM-DE interaction. We note that matter-radiation equality in this case occurs at around $z_{\text{eq}} \sim 3390$ consistent with Planck's measurements. Larger values of ϕ_{ini} lead to larger $\Omega_{\phi 0}$ and thus smaller $\Omega_{\chi 0}$ so that the closure relation holds. The oscillatory feature in Ω can be explained by examining the second row of panels which show the equation of state (EoS) of DM, DE and the total EoS. At early times, $w_\chi = -1$ and $w_\phi = +1$ and so the ϕ field acts as radiation while the χ field acts as an early DE component for a period of time before the onset of rapid oscillations at around $a \sim 10^{-5}$. Averaging the fast oscillations in χ renders $w_\chi = 0$ and so the χ field eventually dilutes as CDM, i.e., $\rho_\chi \sim a^{-3}$. The imprints of these rapid oscillations are visible as little wiggles in the energy density plots in the left-hand-side of the top panel. The ϕ field, on the other hand, starts off as radiation and as the DE potential rolls down to its minimum, the EoS drops to -1 . The interesting feature here is that similar to χ , the DE field begins to oscillate but at a later time, around $a \sim 10^{-2}$. The difference between the oscillations of the χ

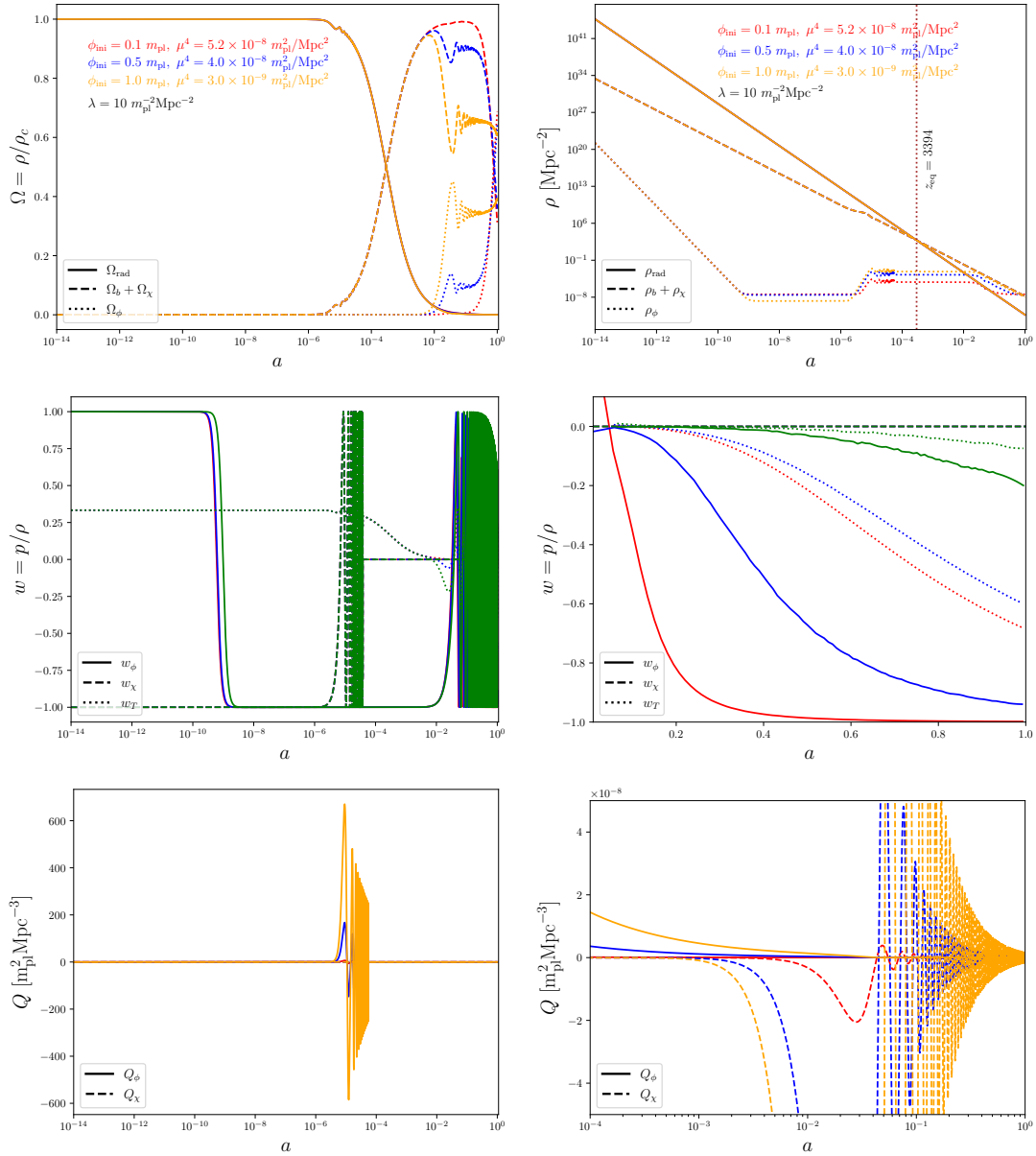


FIG. S1. Results from the first scenario. Top panels: plot of the energy density fractions (left) and the energy densities evolution (right) as a function of the scale factor a . Second row: plot of the evolution of the equations of state (EoS) of DM and DE and the total EoS (left) and a closeup plot on the right for a smaller range of a where a time-average over the oscillations is performed. Third row: plots of the source terms Q_χ and Q_ϕ (left) and a closeup plot on the right. The color code in the top panels is the same for all panels.

and ϕ fields is that while the amplitude of oscillations of w_χ is constant, that of ϕ is decaying. A closer look at these oscillations is exhibited in the right panel where we average over the oscillations for both w_ϕ and w_T . One finds that for $\phi_{\text{ini}} = 0.1$, w_ϕ decays to -1 as one would expect from a DE component, while for $\phi_{\text{ini}} = 0.5$ we get $w_\phi \sim -0.9$. However, for $\phi_{\text{ini}} = 1.0$, the oscillations remain strong even at $a = 1$ and even though the averaged w_ϕ is less than zero, it is still much larger than -1 , which is the well accepted value from observations. Therefore, one can easily reject $\phi_{\text{ini}} = 1.0$ and only consider smaller ϕ_{ini} . Note that even when the oscillations in Ω_χ have been averaged out, they reappear once Ω_ϕ starts its oscillations because the fields are coupled. In the bottom panels of Fig. S1, we show the source terms Q_χ and Q_ϕ over different ranges of a . These terms also show oscillatory patterns over two time scales, similar to w_χ and w_ϕ . In general and at any given time, one of these source terms dominates the other and so

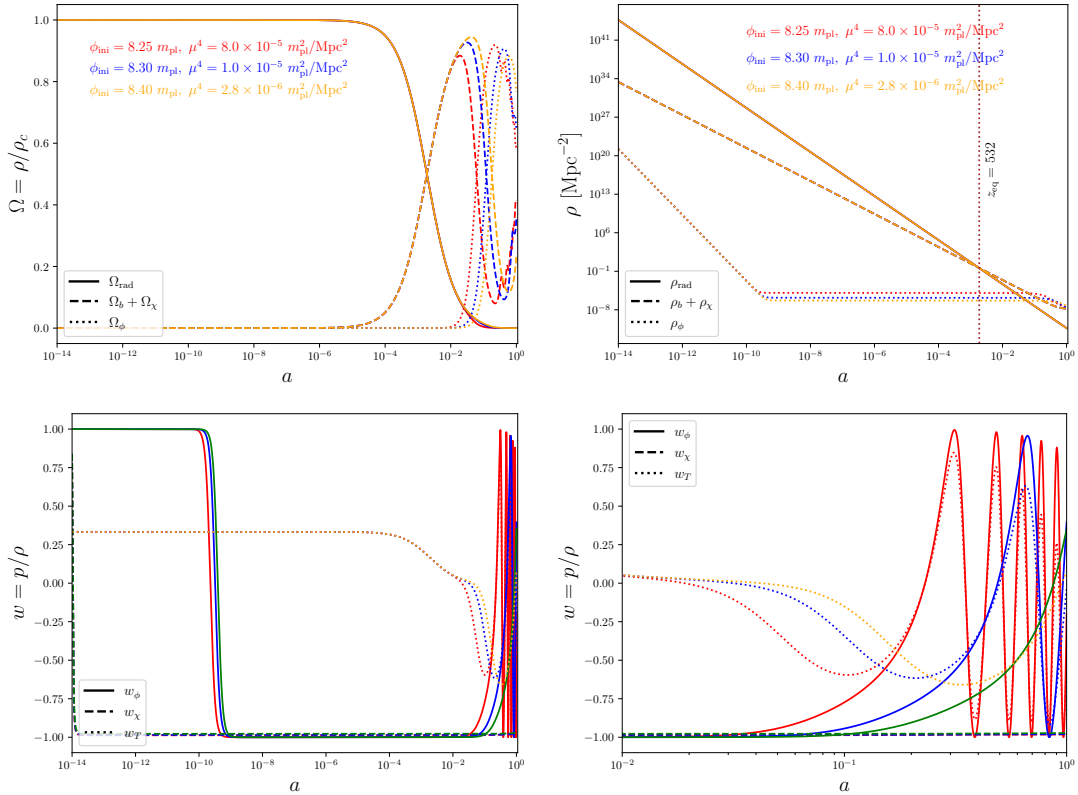


FIG. S2. Results from the second scenario. Plots of the energy density fraction (top left) and the energy density (top right) of all species and the equations of state (EoS) of DM and DE and the total EoS (bottom panels) as a function of the scale factor a . The color code in the top panels is the same for all panels.

one has $Q_\chi + Q_\phi \neq 0$, contrary to the assumption of the phenomenological model.

We now turn to the analysis of the phenomenological model based on the assumption $Q_\chi = -Q_\phi$ in field theory. As a comparison with QCDM, we show the same plots of energy density and equations of state in Fig. S2 and compare them to Fig. S1. The obtained trend is similar to that of normal cosmology but here one can see an important difference relative to the QCDM analysis concerning matter-radiation equality which is attained at $z_{\text{eq}} \sim 532$, in disagreement with Planck's result. Another important difference can also be seen from the evolution of the DM equation of state in the lower left panel of Fig. S2 (dashed line). One can clearly see that the EoS takes a value of -1 throughout the evolution and so the DM field acts as DE. This is the main reason for getting an inconsistent cosmology resulting in a very late matter-radiation equality.

Quintessence transmutation from thawing to scaling freezing

A remarkable consequence of the DM-DE interaction via the field-theoretic interaction term is the transmutation of the quintessence field from thawing to scaling freezing. A characteristic feature of thawing potentials is the departure of the DE equation of state from -1 at late times (close to $a = 1$) while that of scaling freezing potentials is the convergence of the DE equation of state toward -1 close to $a = 1$. In this analysis we have found out that the presence of a DM-DE interaction term of the form $\lambda\chi^2\phi^2/2$ can cause a transmutation from thawing to scaling freezing at some transition scale factor a_t . The secret lies in the behavior of the potential $V_2(\phi) + V_{12}(\phi, \chi)$ close to $a = 1$ where $V_2 + V_{12} \sim \phi^2$ which is exactly the behavior of the scaling freezing double exponential $V_S(\phi) = V(e^{-\lambda_1\phi} + e^{-\lambda_2\phi})$ for $\lambda_1 = -\lambda_2$. We can see this clearly from the right panel of Fig. S3 where the orange curve represent the total potential $V_2(\phi) + V_{12}(\phi, \chi)$ and the blacked dashed curve is the fitting function which has a double exponential form where we found the fit parameters to be $\lambda_1 = -\lambda_2 = -18.2 \text{ m}_{\text{pl}}^{-1}$.

We have also examined the effect of the interaction strength λ on the transition scale factor a_t by running a Monte

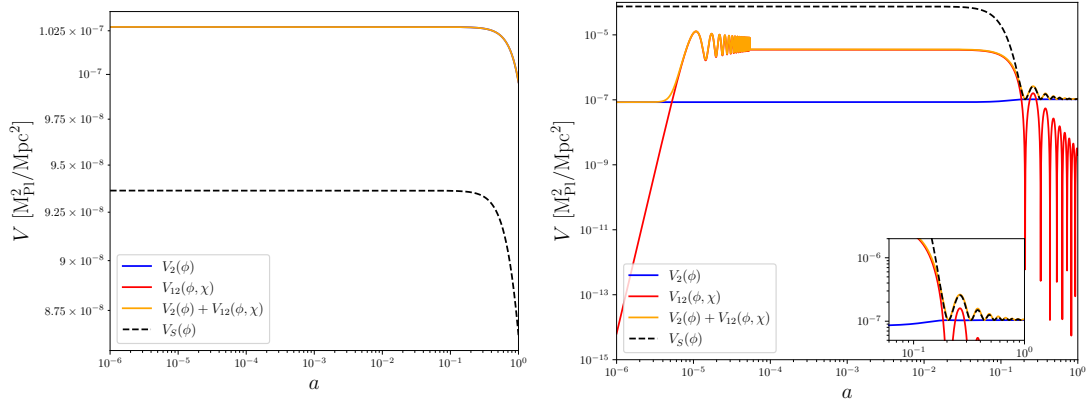


FIG. S3. Left panel versus right panel correspond to the no interaction versus non-zero interaction cases. The evolution of the quintessence potential $V_2(\phi)$ (blue), the interaction potential $V_{12} = \lambda\phi^2\chi^2/2$ (red) and the total potential (orange) as a function of the scale factor a . The potential $V_S(\phi) = V(e^{-\lambda_1\phi} + e^{-\lambda_2\phi})$ (black dashed) is fitted to the total potential, where $\lambda_1 = -\lambda_2 = -18.2 \text{ m}_{\text{pl}}^{-1}$. The fit works very well for $a > 0.1$ (inset of right panel).

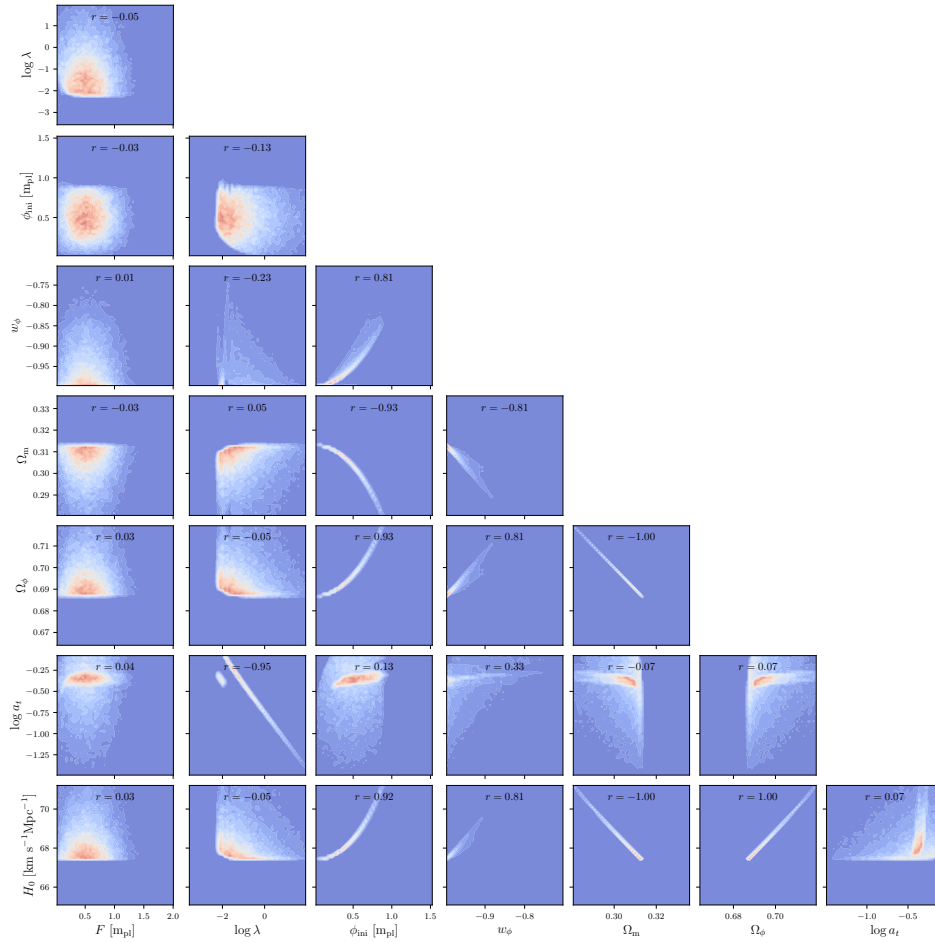


FIG. S4. Density plots of the input parameters (F , λ , ϕ_{ini}) and the corresponding output quantities (EoS w_ϕ , matter and DE density fractions Ω_m and Ω_ϕ , today's Hubble parameter H_0 and the scale factor a_t corresponding to the transition between thawing and scaling freezing quintessence) and their correlations. There is a strong positive correlation between H_0 and ϕ_{ini} ($r = 0.92$) and a strong negative correlation between a_t and λ ($r = -0.94$). The latter suggests that the interaction strength indeed causes a switch between the two quintessence models.

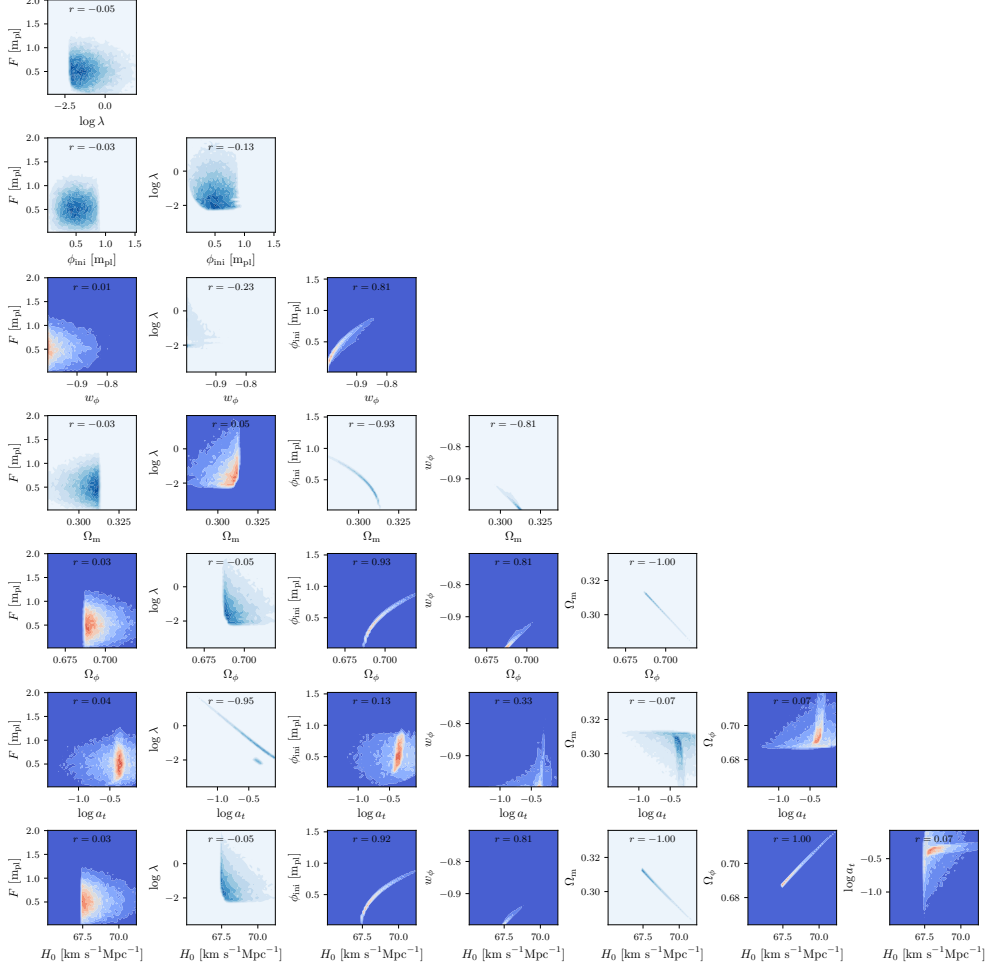


FIG. S5. Pair-wise density plots of the input parameters (F , λ , ϕ_{ini}) and the corresponding output quantities (EoS w_ϕ , matter and DE density fractions Ω_m and Ω_ϕ , today's Hubble parameter H_0 and the scale factor a_t corresponding to the transition between thawing and scaling freezing quintessence) and their correlations. There is a strong positive correlation between H_0 and ϕ_{ini} ($r = 0.92$) and a strong negative correlation ($r = -0.94$) between a_t and λ . The latter suggests that the interaction strength indeed causes a switch between the two quintessence models.

Carlo analysis of the model. In Figs. S4 and S5, we show the correlation plots between the different parameters of the model. From Fig. S4, it is clear that a_t and λ are strongly anti-correlated which means that a stronger interaction results in an earlier transition between the two quintessence states. As discussed in the Letter, such a transition can be searched for in the data and its detection would provide a direct evidence of a dark energy and dark matter interaction.